

CHAPTER 236

SIMULATION OF COASTAL PROFILE DEVELOPMENT USING A BOUSSINESQ WAVE MODEL

K.A. Rakha¹, R. Deigaard², P.A. Madsen¹, I. Brøker³, and J.K. Rønberg³

ABSTRACT

A phase-resolving wave transformation module is combined with an intra-wave sediment transport module to calculate the on/offshore sediment transport rates. The wave module is based on the Boussinesq equations extended into the surf zone. The vertical variation of the instantaneous currents and concentrations are calculated. The net sediment transport rates are calculated, and the equation for conservation of sediment is solved to predict the beach profile evolution. The results of the present paper showed that the undertow contribution to the sediment transport rates dominated only at local areas even for eroding beaches, suggesting that other contributions should not be neglected.

1. INTRODUCTION

The study of beach profile evolution includes a large range of time and space scales. Process based morphology models (Roelvink and Brøker, 1993) usually include some averaging of the different space and time scales. This averaging is applied to either the hydrodynamic or the sediment transport calculations or both. The sediment transport calculations used in most of the present morphology models are based on phase-averaged calculations of the sediment concentrations or on the 'energetics approach'. Although models based on the energetics approach account for the intra-wave sediment transport rates, the intra-wave variation of the eddy viscosities and sediment concentrations are not calculated. Such models may be classified as semi-intra-wave sediment transport models. The model developed by Fredsøe et al. (1985) represents an example of a detailed intra-wave model for the sediment concentrations. Watanabe (1994) combined a wave model based on the Boussinesq equations with a semi-intra-wave sediment transport model. Such a model neglects a large part of the information provided by the wave module, and will require some approximations for irregular waves. The model described by Brøker et al. (1991) combines a detailed intra-wave sediment transport module with a phase-averaged wave module, where a wave theory is required to describe the intra-wave water motion. The extension of such a model to irregular waves will also require some approximations. In the present study a phase-resolving wave module is combined with a detailed intra-wave sediment transport module to study in more detail the process of sediment transport and morphological evolution.

¹International Research Center for Computational Hydrodynamics (ICCH)

Danish Hydraulic Institute (DHI), Agern Allé 5, DK-2970 Horsholm, Denmark.

* Currently at Department of Irrigation and Hydraulics, Faculty of Eng., Cairo University, Egypt.

²Institute of Hydrodynamics and Hydraulic Eng. (ISVA), Technical University of Denmark, DK-2800 Lyngby, Denmark.

³Danish Hydraulic Institute (DHI), Agern Allé 5, DK-2970 Horsholm, Denmark.

2. MODEL DESCRIPTION

The morphological calculations are performed by updating the beach profile over the morphological time step Δt_{\max} . For each morphological update the simulations are performed by four modules; a wave module, a hydrodynamic module, a sediment transport module and a bathymetry updating module.

2.1 Wave Module

The wave module simulates the wave conditions across the beach profile by a phase-resolving model based on the Boussinesq equations, with improved linear dispersion characteristics as explained in Madsen et al. (1991), and Madsen and Sørensen (1992). The effect of wave breaking is included by using the surface roller concept (Schäffer et al., 1993). Figure (1A) shows a sketch of the assumed velocity field under a wave with a surface roller. An extra term is included in the momentum equation to represent the momentum flux due to the rollers. This term extracts energy from the wave motion. Breaking is initiated when the local water surface slope exceeds the initial value of ϕ_b . The roller is defined as the water above the tangent slope $\tan(\phi)$. Initially ϕ is equal to ϕ_b for each roller, which then decreases exponentially to ϕ_o , and breaking is assumed to cease when the maximum of the local slope becomes less than $\tan(\phi)$. The resulting roller thickness δ is finally multiplied by the roller shape factor f_δ to compensate for the simple method of separating the roller from the rest of the flow.

The calculation proceeds into the swash zone using the slot-technique (Madsen et al. 1994), by extending the computational domain into an artificial permeable beach. Near the moving shoreline the water surface will intersect with the sea bed and continue into the porous beach. The instantaneous position of the shoreline is simply determined by this intersection.

2.2 Hydrodynamic Module

The hydrodynamic module consists of two parts, an oscillatory boundary layer model (Figure, 1B) and an undertow model (Figure, 1C). The boundary layer model calculates the vertical velocity distribution for the oscillatory wave motion u_o inside the boundary layer. The undertow model determines the vertical distribution of the mean undertow \bar{U}_o .

2.2.1 Boundary Layer Calculations

The oscillatory flow near the bottom is modelled by the momentum integral method developed by Fredsoe (1984). The shear stress is assumed to be zero at the top of the boundary layer, and the velocity distribution u inside the boundary layer is assumed to follow a logarithmic distribution. The boundary layer thickness is assumed to develop from zero at every zero-crossing of u_o outside the boundary layer. The values of the shear velocity U and the boundary layer thickness ζ are calculated for each time step. The streaming in the boundary layer and the wave asymmetry causes the time averaged bed shear stress to deviate from zero. To obtain this mean shear stress a constant drift velocity V_{st} is added to the near bed orbital velocity. The magnitude of V_{st} is found by iteration requiring that the time averaged bed shear stress in the boundary layer model is equal to the shear stress determined by the streaming.

2.2.2 Eddy Viscosity Calculations

The eddy viscosities are calculated by assuming that the total kinetic energy can be determined as the sum of three contributions (Brøker et al., 1991),

$$\epsilon = \sqrt{\epsilon_w^2 + \epsilon_b^2 + \epsilon_U^2} \quad (1)$$

where, ϵ_w , ϵ_b , and ϵ_U are the eddy viscosities due to the bottom boundary layer, wave breaking, and the undertow, respectively. The eddy viscosity ϵ_w is calculated based on the variables calculated in

the boundary layer, assuming a parabolic distribution inside the bottom boundary layer (Fredsøe et al., 1985). The eddy viscosity ϵ_v is calculated from the undertow velocity profile using a simple mixing length formulation. The eddy viscosity ϵ_b is calculated from the turbulent kinetic energy induced by wave breaking calculated from a one-equation turbulence model (Deigaard et al. 1991). The instantaneous production of turbulence due to wave breaking is calculated from the following equation proposed by Deigaard (1989),

$$P_r = \alpha_p Diss = \alpha_p \rho g c \delta \tan \phi_o \quad (2)$$

where, Diss is the instantaneous energy dissipation due to wave breaking, and α_p is the fraction of the energy that is not dissipated immediately in the shear layer beneath the roller. α_p is assumed to be 0.33 as suggested by Deigaard et al. (1991). The production of turbulence is assumed to have a parabolic distribution over a distance of half the wave height ($H/2$) below the mean water depth as shown in Figure (2).

2.2.3 Undertow Calculation

The undertow is calculated by the following approximate equation,

$$\frac{\partial U_c}{\partial y} = \frac{1}{\rho \epsilon} \bar{\tau} \quad (3)$$

where an overbar denotes time averaging over a single wave. The time averaged shear stress distribution is assumed to vary linearly over the water depth as shown in Figure (2). The shear stress at the surface (mean water level, MWL) is calculated from the following formula,

$$\bar{\tau}_s = \frac{Diss}{c} \quad (4)$$

Eqn. (3) is solved with the no slip condition imposed at the bed, and the condition that the total flux compensates the wave drift (determined from the Boussinesq model) and the velocity V_{st} determined by the boundary layer model.

2.3 Sediment Transport Module

2.3.1 Bed Load and Sediment Concentrations

The instantaneous near bed concentration C_b is calculated from the formulation suggested by Zyserman and Fredsøe (1994). The value of C_b depends on the instantaneous value of the Shield's parameter. The instantaneous bed load q_b is calculated using the formulation by Engelund and Fredsøe (1976).

Neglecting the convective terms, the distribution of the sediment concentration C can be calculated from the diffusion equation,

$$\frac{\partial C}{\partial t} = w_f \frac{\partial C}{\partial y} + \frac{\partial}{\partial y} \left(\epsilon_s \frac{\partial C}{\partial y} \right) \quad (5)$$

where, ϵ_s is the sediment diffusion coefficient assumed to be the same as the flow eddy viscosity ϵ , and w_f is the fall velocity. Eqn. (5) is solved with the boundary conditions $C = C_b$ at the bed ($y = 2D_{50}$), and zero sediment flux through the water surface.

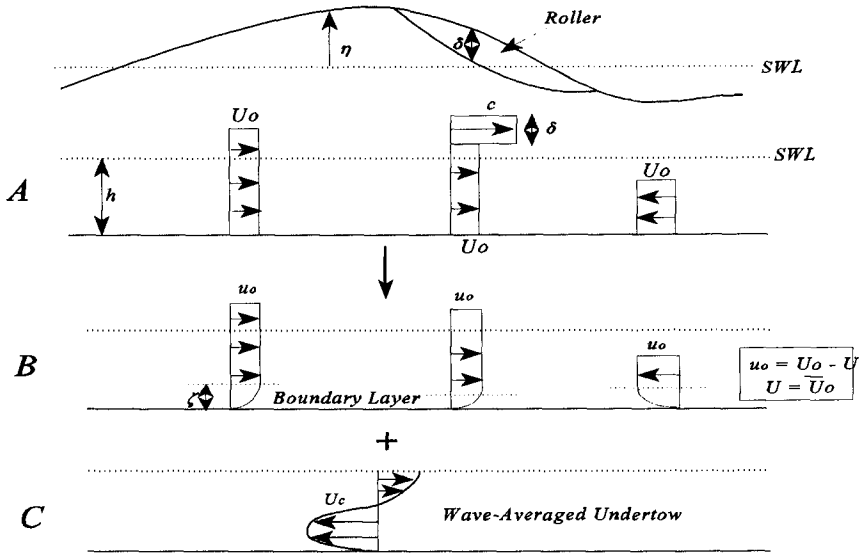


Figure (1): The elements of the hydrodynamic module; A- The wave description. B- The oscillatory current. C- The undertow.

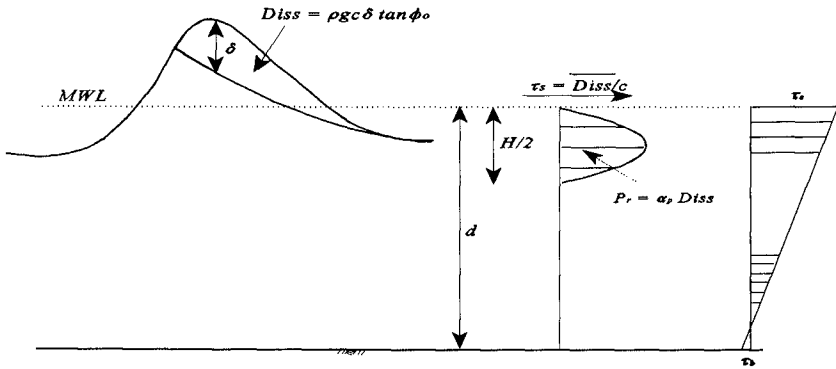


Figure (2): Vertical distribution of production of turbulence and shear stresses due to wave breaking.

2.3.2 Lagrangian Drift

For an Eulerian calculation a contribution due to the Lagrangian drift should be added as an approximation for the wave drift of suspended sediment (Brøker et al., 1991). This approximation is required because the convective terms were not included in the calculations for the sediment concentrations. The Lagrangian drift velocity U_l results from the fact that the water particles do not follow a closed path, but a net forward displacement exists. As an approximation it is assumed that the sediment on average follows the fluid motion. The drift current for each wave is calculated from,

$$U_l = \frac{1}{c} \left(\overline{u^2} - (\bar{u})^2 \right) \quad (6)$$

where an overbar again denotes time averaging over a single wave.

2.3.3 Total Sediment Transport Rates

The total instantaneous sediment transport rates are obtained from,

$$q'_s = q_b + q_{sw} + q_{su} + q_{sl} \quad (7)$$

where the sediment transport rates due to the oscillatory motion q_{sw} are evaluated by integrating uC over the water depth. The contributions due to the undertow q_{su} and the Lagrangian drift q_l are evaluated by integrating $U_c C$ and $U_l C$ over the water depth respectively. The swash zone was included in an approximate manner by assuming that q'_s varies linearly from the last grid point to the location of the water line for each time step. Time averaging of q'_s over the time series provides the time averaged sediment transport rates q_s . Figure (3) shows the instantaneous sediment transport rates calculated for a regular and irregular wave of the same deep water rms wave height for Test 1c explained later. As shown in Figure (3) the time variation of the sediment transport rates under an irregular wave are quite different from a "representative" regular wave.

2.4 MORPHOLOGY MODULE

The bathymetry is updated by solving the conservation of sediment equation,

$$\frac{\partial Z_b}{\partial t} = -\frac{1}{(1-n)} \frac{\partial q_s}{\partial x} \quad (8)$$

where Z_b is the bed level, and n is the porosity of the sediment assumed to be 0.4. A Forward in Time Central in Space (FTCS) finite difference scheme was used to solve Eqn. (8), with an additional diffusive term for the numerical stability (Abbott and Basco, 1989). The resulting finite difference equation would correspond to the following differential equation,

$$\frac{\partial Z_b}{\partial t} + \frac{1}{(1-n)} \frac{\partial q_s}{\partial Z_b} \frac{\partial Z_b}{\partial x} = K \frac{\partial^2 Z_b}{\partial x^2} \quad (9)$$

where, K is a diffusion coefficient assumed to be proportional to q_s ,

$$K = \epsilon_s |q_s| \quad (10)$$

which is similar to the additional gravitational term included by De Vriend et al. (1993) and

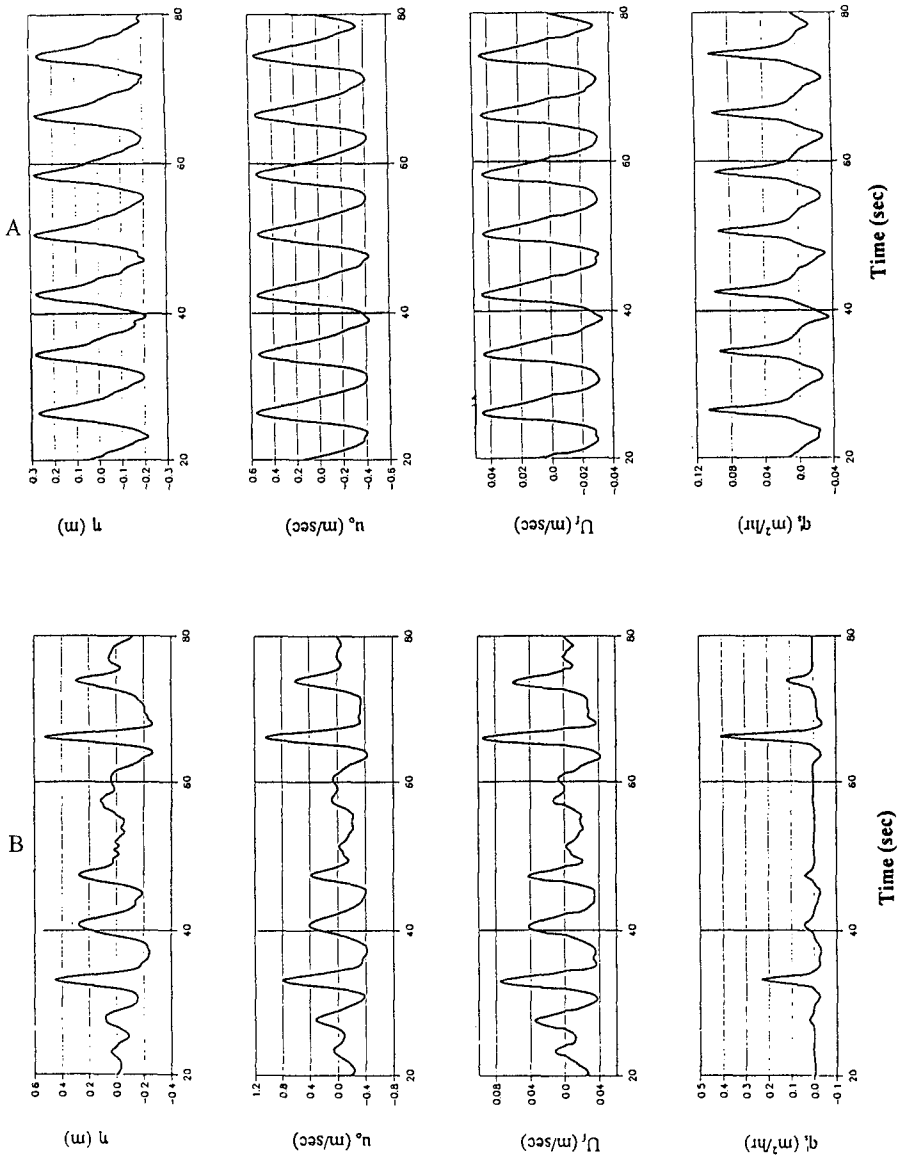


Figure (3): A- Time series of η , u_o , U_r , and q_r of Test 1c (regular wave).
 B- Time series of η , u_o , U_r , and q_r of Test 1c (irregular wave).

Horikawa (1988). ϵ_s is an empirical coefficient. The following constraint on the morphological time step Δt must be satisfied (Abbott and Basco, 1989),

$$D_{cr} \leq \frac{1}{2} ; D_{cr} = \frac{K\Delta t}{\Delta x^2} \tag{11}$$

where, Δx is the spatial grid spacing. In the present study two time steps are used; the first is called the inner time step Δt_i and the second the outer time step Δt_{max} . The maximum value of Δt_i is chosen to satisfy Eqn. (11). Eqn. (8) is solved over the duration Δt_{max} with the values of q assumed constant (Horikawa, 1988, and Rakha and Kamphuis, 1996). The value of Δt_{max} was specified to the model together with a criterion limiting the maximum change in bed level to 10% of the deep water average wave height (Rakha et al., 1996). A modified Lax-Scheme (Abbott, 1979) with no inner times steps was also tested.

Figure (4) shows a long term simulation for a highly erosive beach with a specified outer time step $\Delta t_{max} = 0.2$ hr. The actual time step was less than 0.1 hr resulting in nearly 80 wave field updates. As shown in Figure (4) the bars tended to move offshore with the depth over their crests increasing with time. Onshore of the previous bar, new bars also developed with time.

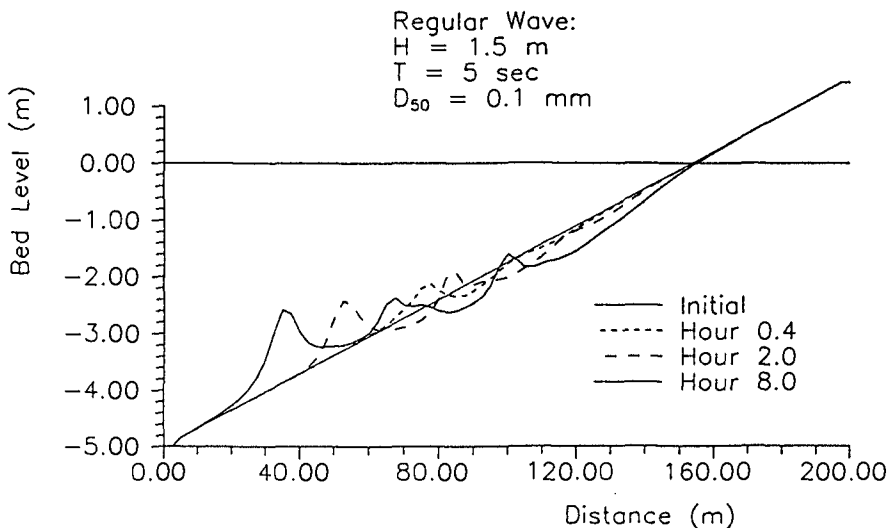


Figure (4): Long term morphology simulation for a regular wave.

3. MODEL VALIDATION

3.1 LIP 11D Delta Flume Tests

The Delta Flume '93 tests were performed at the Delft Hydraulics large-scale wave flume. These tests were supported by the "Large Installations Plan" (LIP) of the European Union. The main purpose of the tests was to provide high quality data to validate/calibrate numerical beach profile models. The details of the tests performed can be found in Arcilla et al. (1993) and Roelvink and Reniers (1995). Two tests (Tests 1b and 1c) were selected for the model verification. Test 1b represents a highly erosive wave condition, and Test 1c a strongly accretive wave condition. Table (1) provides a summary of the test conditions used in this paper.

Table (1): Summary of Test Conditions.

Test	H_{m0} (m)	T_p (sec)	D_{s0} (mm)	Type
LIP 11D: Test 1c	0.60	8.0	0.2	Irregular
LIP 11D: Test 1b	1.40	5.0	0.2	Irregular
Shimizu et al. (1985): Test 3-2	1.05	6.0	0.27	Regular

The prediction of the characteristic wave height H_{m0} variation over the initial bathymetry for Tests 1c and 1b is shown in Figures (5) and (6) respectively. The Boussinesq model predicted the wave heights well for both Tests. It appears that the wave heights are slightly overpredicted inside the surf zone for Test 1c (Figure, 5). The results obtained using a phase-averaged wave model based on the Battjes and Janssen (1978) model are also shown in both figures, which shows that such a model provides a good estimate for H_{m0} .

Figures (7) and (8) show the time-averaged undertow for Tests 1c and 1b. At some locations measurements were performed twice at different hours of the test. Figures (7) and (8) show that the undertow is predicted well for most sections. The undertow however is overpredicted just before the bar ($x = 138$) for Test 1c and underpredicted in the trough of the bar ($x = 145$) for both Tests 1b and 1c.

The predicted on/offshore sediment transport rates for Test 1c are shown in Figure (5). Very good results are obtained outside the surf zone showing that the calculation of the sediment transport rates due to the oscillatory current is well predicted. Over the bar, the overestimation of the undertow (Figure, 8) results in the underestimation of the onshore sediment transport rates. Good predictions of the sediment transport rates for Test 1b are also shown in Figure (6), where the model follows the measured sediment transport rates well. The onshore sediment transport rates are overestimated inside the trough of the bar ($x = 145$) due to the underestimation of the undertow as explained earlier (Figure, 8). The use of the Boussinesq model provided much better results than the use of a phase-averaged wave model (Figures, 5 & 6). Linear wave theory was used with the rms wave height assumed to be the representative wave for the phase-averaged wave model calculations.

Figure (9) shows a decomposition of the time averaged sediment transport rates into three of the four calculated components. The three contributions plotted are the Lagrangian drift, the integral of uC , and the contribution due to the undertow. The bed load was not included since it gives only a small contribution for these tests. From Figure (9) it can be seen that for Test 1c just before the bar where some of the waves start breaking, the undertow contribution increases rapidly. The measurements suggest that the drop in the sediment transport rates is delayed and occurs on the top of the bar. Figure (9) shows that for eroding beaches (Test 1b) the contributions due to the oscillatory current and the Lagrangian drift are important. The undertow contribution dominates only at the locations where a high percentage of waves are breaking.

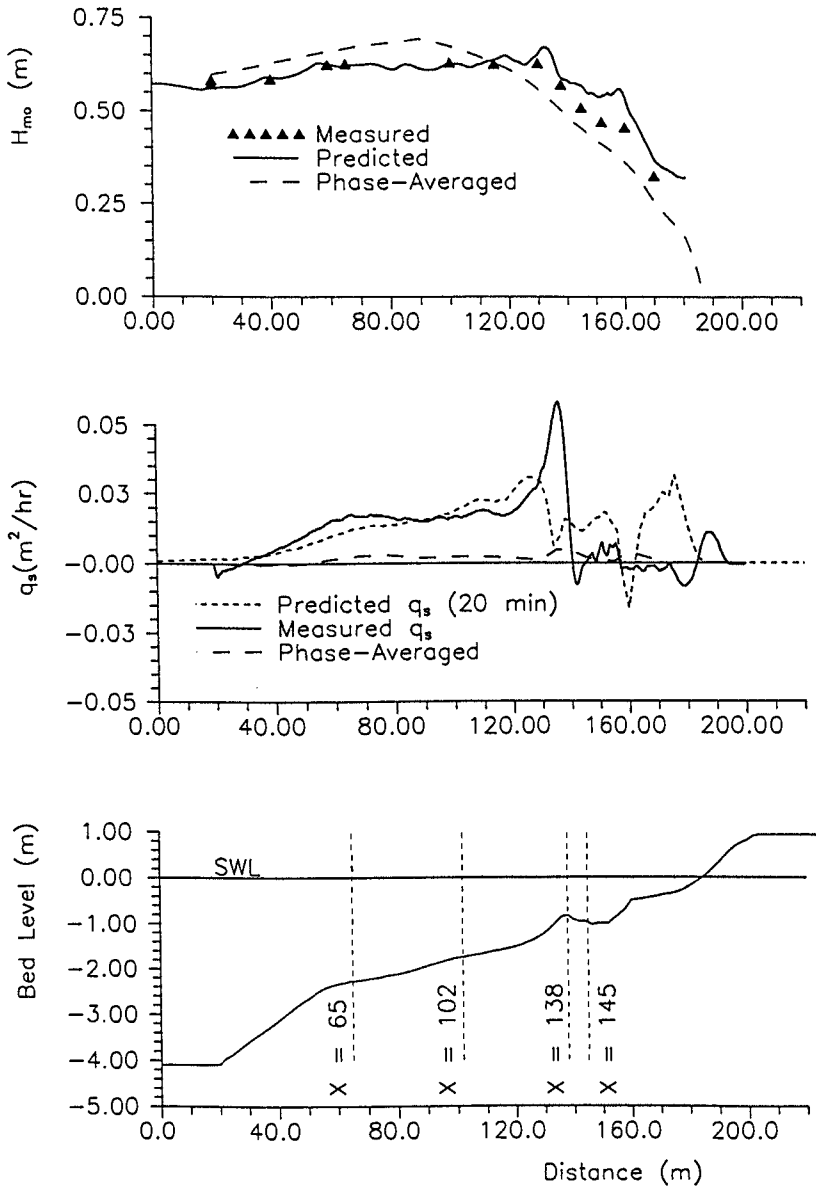


Figure (5): Model results for H_{mo} and q_s of Test 1c (LIP 11D).

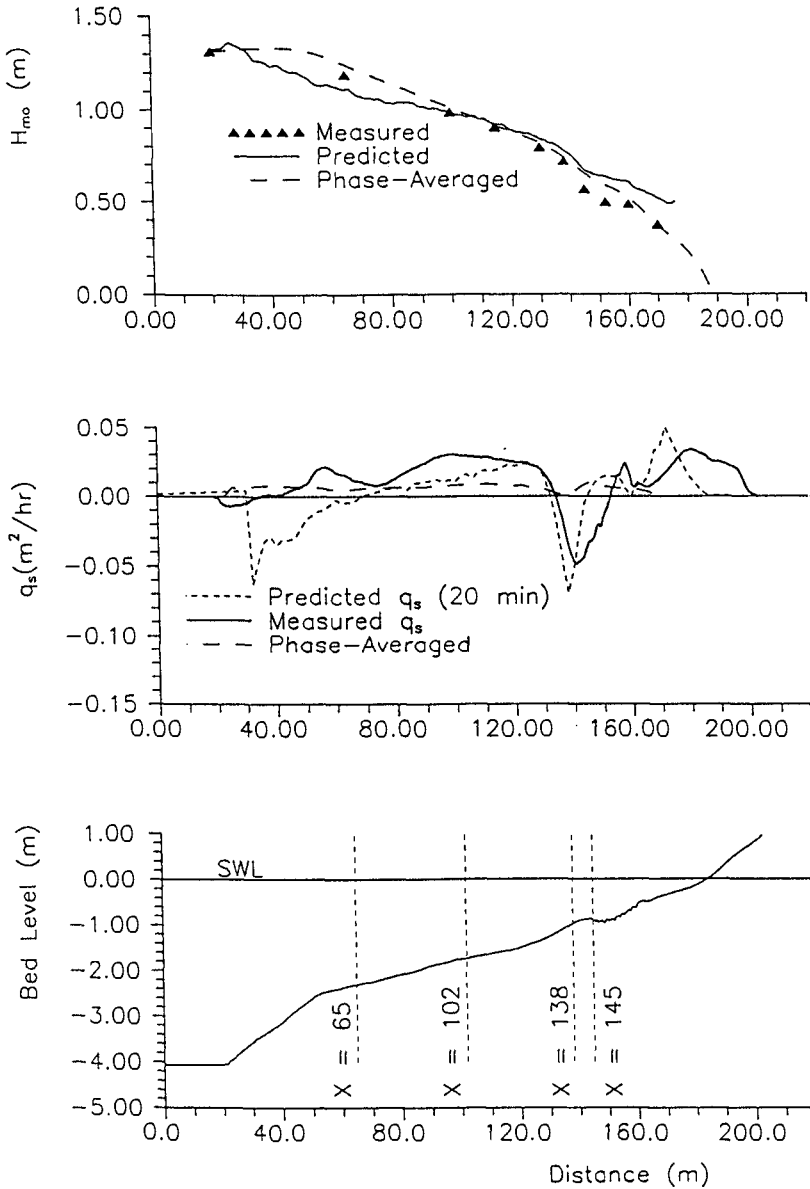


Figure (6): Model results for H_{mo} and q_s of Test Ib (LIP IID).

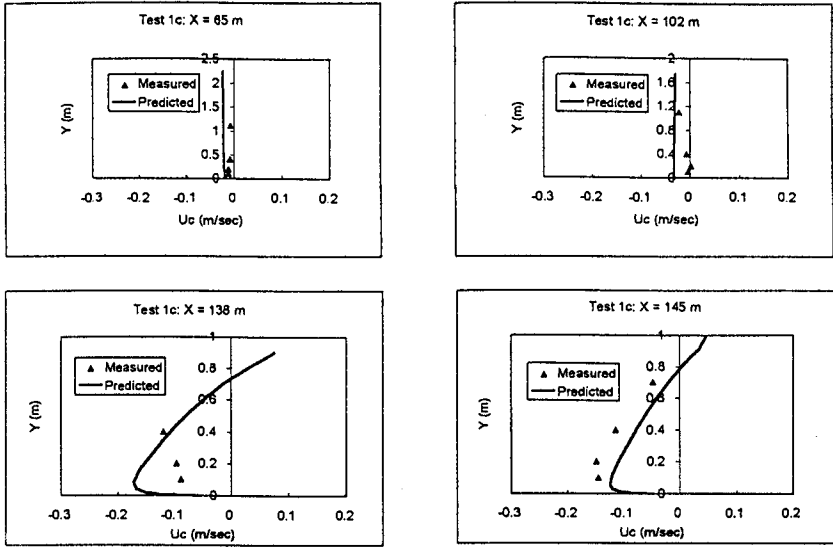


Figure (7): Model results for Undertow of Test 1c (LIP 11D).

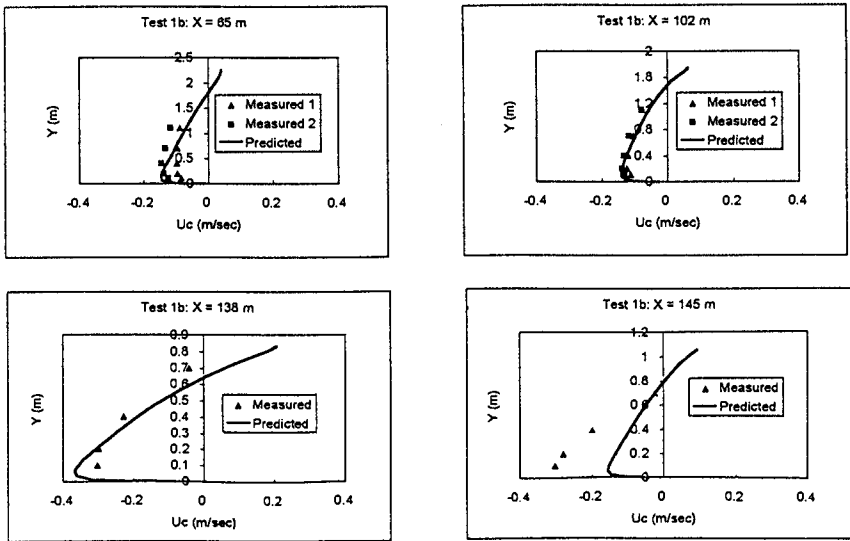


Figure (8): Model results for Undertow of Test 1b (LIP 11D).

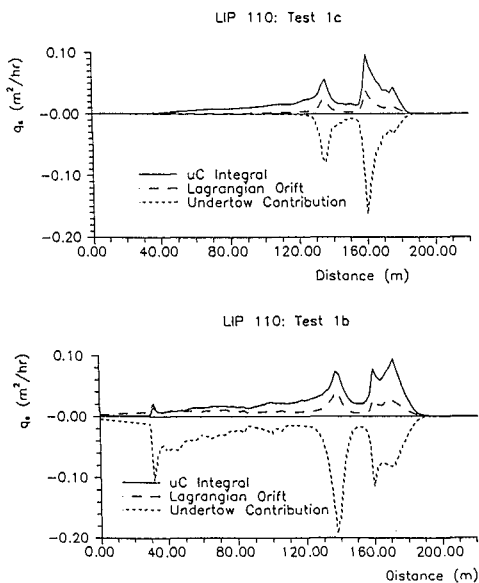


Figure (9): Sediment transport rate contributions for Tests 1c and 1b (LIP 11D).

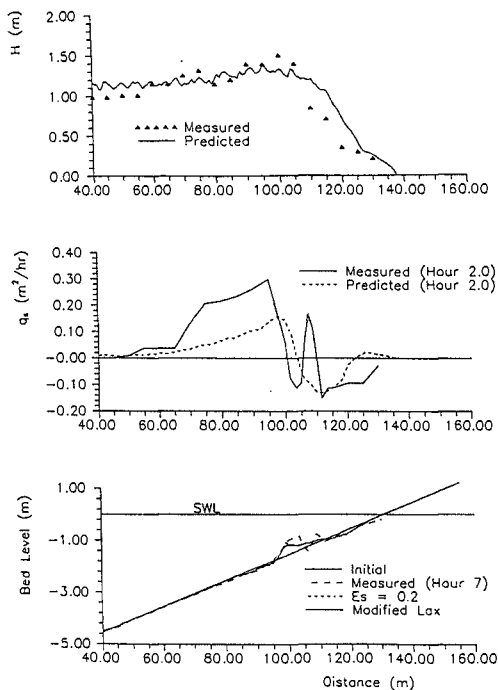


Figure (10): Model results for Test 3-2 (Shimizu et al., 1985).

3.2 Validation of Morphology Model

Figure (10) shows the morphology model predictions for Test 3-2 of Shimizu et al. (1985) with the test conditions provided in Table (1). Good results were obtained for the bar formation as shown in Figure (10) although the numerical model underpredicted the bar development due to the underprediction of the sediment transport rates outside the surf zone. Figure (10) shows that the Boussinesq model underpredicts the shoaling of the waves outside the surf zone. This underprediction of the wave shoaling could be responsible for the underprediction of the sediment transport rates. As shown in Figure (10) the modified Lax-scheme and the FTCS scheme with $\epsilon_s = 0.2$ gave similar results. A sensitivity analysis on the effect of using a value of $\epsilon_s = 2.0$ (as suggested by Watanabe, 1994) showed that the model was not sensitive to the value of ϵ_s for this case.

CONCLUSIONS

A phase-resolving wave transformation module was combined with an intra-wave sediment transport module to predict the on/offshore sediment transport rates and the resulting beach evolution. The roller geometry was used to determine the instantaneous production of turbulence and a mean shear stress at the water surface. The instantaneous sediment transport rates due to the oscillatory wave induced currents (bed load and suspended load), the undertow, and the Lagrangian drift were calculated.

The present model was verified against a few test conditions. The model predicted the undertow and the sediment transport rates well for both erosive and accretive conditions. The onshore sediment transport rates for accretive beaches were underpredicted before the bar due to the overprediction of the undertow, and the underprediction of wave shoaling.

The results of the present paper showed that even for eroding beaches the undertow contribution to the sediment transport rates dominated only at local areas, suggesting that other contributions should not be neglected for eroding beaches.

ACKNOWLEDGMENT

The Danish National Research Foundation financed the first and third authors and the Danish Technical Research Council under the program 'Marin Teknik' financed the fourth author, their support is greatly appreciated. The assistance of Ole Sørensen with the Boussinesq model is also appreciated. Dano Roelvink (Delft Hydraulics) helped in providing the data for the LIP experiments.

REFERENCES

- Abbott, M.B. (1979). *Computational Hydraulics*. Pitman Books Ltd.
- Abbott, M.B. and Basco, D.R. (1989). *Computational Fluid Dynamics*. John Wiley and Sons, Inc., New York. 425p.
- Arcilla, A.S., Roelvink, J.A., O'Conner, B.A., Reniers, A., and Jimenez, J.A. (1994). The Delta Flume '93 experiment. *Coastal Dynamics 1994*, ASCE, Barcelona, pp. 488-502.
- Battjes, J.A. and Janssen, J.P.F.M. (1978). Energy loss and set-up due to breaking of random waves. *Proc. 16th Int. Conf. Coastal Eng., ASCE, Vol. I*, pp. 569-589.
- Brøker, H.I., Deigaard, R., and Fredsøe, J. (1991). On/offshore sediment transport and morphological modelling of coastal profiles. *Proc. ASCE Specialty Conf. Coastal Sediments' 91*, Seattle, WA, pp. 643-657.
- Deigaard, R., (1989). *Mathematical modelling of waves in the surf zone*. Progress Report 69, ISVA, Technical University, Lyngby, Denmark, pp. 47-59.
- Deigaard, R., Justesen P., and Fredsøe, J. (1991). Modelling of undertow by a one-equation turbulence model. *Coast. Eng., Vol.15*, pp.431-458.

- De Vriend, H.J., Zyserman, J., Nicholson, J., Roelvink, J.A., Péchon, P., and Southgate, H.N. (1993). Medium-term 2DH coastal area modelling. *Coast. Eng.*, Vol.21, pp.193-224.
- Engelund, F., and Fredsøe, J. (1976). A sediment transport model for straight alluvial channels. *Nordic Hydrology*, Vol. 7, pp. 293-306.
- Fredsøe, J. (1984). The turbulent boundary layer in combined wave current motion. *Journal of Hydraulic Eng.*, ASCE, Vol. 110, No.HY8, pp. 1103-1120.
- Fredsøe, J., Andersen, O.H., and Silberg, S. (1985). Distribution of suspended sediment in large waves. *Journal of Waterway, Port, Coastal and Ocean Eng.*, ASCE, Vol. 111, No. 6, pp. 1041-1059.
- Fredsøe, J., and Deigaard, R. (1992). *Mechanics of Coastal Sediment Transport*. World Scientific, 369p.
- Horikawa, K. (1988). *Nearshore dynamics and coastal processes*. University of Tokyo Press.
- Madsen, P.A., Murray, R., and Sørensen (1991). A new form of the Boussinesq equations with improved linear dispersion characteristics. *Coast. Eng.*, Vol.15, pp.371-389.
- Madsen, P.A., Sørensen O.R. (1992). A new form of the Boussinesq equations with improved linear dispersion characteristics. Part 2. A slowly-varying bathymetry. *Coast. Eng.*, Vol.18, pp.183-204.
- Madsen, P.A., Sørensen O.R., Schäffer, H.A. (1994). Time domain modelling of wave breaking, runup, and surf beats. 24th Int. Conf. on coastal Eng., pp. 399-411.
- Rakha, K.A., and Kamphuis, J.W. (1996). A morphology model for an eroding beach backed by a seawall. Submitted to *Coastal Eng.*
- Rakha, K.A., Deigaard, R., Brøker, I. (1996). A phase-resolving cross shore sediment transport model for beach profile evolution. Submitted to *Coastal Eng.*
- Roelvink, J.A. and Brøker, I. (1993). Cross-shore profile models. *Coast. Eng.*, ASCE, Vol.21, pp.163-191.
- Roelvink, J.A. and Reniers, A.J.H.M. (1995). LIP 11D delta flume experiments. Data Report, Delft Hydraulics, H 2130.
- Schäffer, H.A., Madsen, P.A., and Deigaard, R. (1993). A Boussinesq model for waves breaking in shallow water. *Coastal Eng.*, Vol. 20: 185-202.
- Shimizu, T., Sato, S., Maruyama, K., Hasegawa, H., and Kajima, R. (1985). Modeling of cross-shore sediment transport rate distributions in a large wave flume, Report of Central Res. Inst. for Electric Power Industry, Rep. No. 384028, 60 p. (in Japanese).
- Watanabe, A. (1994). A mathematical model of beach processes under sheet-flow condition using nonlinear wave theory. *International Symposium Waves - Physical and Numerical Modelling*, Vancouver, Canada, pp.1520-1529.
- Zyserman, J.A. and Fredsøe, J. (1994). Data analysis of bed concentration of suspended sediment. *Journal of Hydr. Engrg.*, ASCE, 120(9).